



The Thomas Jefferson National Accelerator Facility
Theory Group Preprint Series

Additional copies are available from the authors.

The Southeastern Universities Research Association (SURA) operates the Thomas Jefferson National Accelerator Facility for the United States Department of Energy under contract DE-AC05-84ER40150.

DISCLAIMER

This report was prepared as an account of work sponsored by the United States government. Neither the United States nor the United States Department of Energy, nor any of their employees, makes any warranty, expressed or implied, or assumes any legal liability or responsibility for the accuracy, completeness, or usefulness of any information, apparatus, product, or process disclosed, or represents that its use would not infringe privately owned rights. Reference herein to any specific commercial product, process, or service by trade name, mark, manufacturer, or otherwise, does not necessarily constitute or imply its endorsement, recommendation, or favoring by the United States government or any agency thereof. The views and opinions of authors expressed herein do not necessarily state or reflect those of the United States government or any agency thereof.

JLAB-THY-00-03
ZTF-99/13

Anomalous $\gamma \rightarrow 3\pi$ amplitude in a bound-state approach

Bojan Bistrović

Physics Department, Old Dominion University, 4600 Elkhorn Avenue, Norfolk, VA 23529, U.S.A.,
and Jefferson Lab, 12000 Jefferson Avenue, Newport News, VA 23606, U.S.A.

Dubravko Klabučar

Physics Department, Faculty of Science, Zagreb University, Bijenička c. 32, 10000 Zagreb, Croatia

Abstract

The form factor for the anomalous process $\gamma\pi^+ \rightarrow \pi^+\pi^0$, which is presently being measured at CEBAF, is calculated in the Schwinger-Dyson approach in conjunction with an impulse approximation. The form factors obtained by us are compared with the ones predicted by the simple constituent quark loop model, vector meson dominance and chiral perturbation theory, as well as the scarce already available data.

PACS: 13.40.Gp 12.38.Lg 14.40.Aq 24.85.+p

Keywords: Chiral symmetry breaking, Constituent quarks, Nonperturbative QCD and hadron phenomenology, Schwinger-Dyson equations

1. The Schwinger-Dyson (SD) approach to the physics of quarks and hadrons (see [1,2] for reviews) provides one with a modern constituent quark model possessing many remarkable features. Its presently interesting feature is its relation with the Abelian axial anomaly. Other bound state approaches generally have problems with describing anomalous processes such as the $\pi^0 \rightarrow \gamma\gamma$ decay. (See [3] for a comparative discussion thereof.) It was therefore a significant advance in the theory of bound states, when Roberts [4] and Bando *et al.* [5] showed that the SD approach reproduces exactly (in the chiral and soft limit of pions of vanishing pion mass m_π) the famous anomalous $\pi^0 \rightarrow \gamma\gamma$ "triangle"-amplitude $T_\pi^{2\gamma}(m_\pi = 0) = e^2 N_c / (12\pi^2 f_\pi)$, and when Alkofer and Roberts (AR) [6] reproduced the anomalous "box"-amplitude for the $\gamma \rightarrow \pi^+\pi^0\pi^-$ process, in the same approach and limits. They obtained the form factor $F_\gamma^{3\pi}(p_1, p_2, p_3)$ at the soft point, where the momenta of all three pions $\{p_1, p_2, p_3\} \equiv \{p_{\pi^+}, p_{\pi^0}, p_{\pi^-}\}$ vanish

$$F_\gamma^{3\pi}(0, 0, 0) = \frac{1}{ef_\pi^2} T_\pi^{2\gamma}(0) = \frac{eN_c}{12\pi^2 f_\pi^3}, \quad (1)$$

as predicted on fundamental grounds by Adler *et al.*, Terent'ev, and Aviv and Zee [7] (the number of quark colors is $N_c = 3$, while e denotes the proton charge, and f_π the pion decay constant).

Just as the triangle amplitude $T_\pi^{2\gamma}(0)$, the anomalous box amplitude (1) is in the SD approach evaluated analytically and without any fine tuning of the bound-state description of the pions [6].

This happens because the SD approach incorporates the dynamical chiral symmetry breaking (D χ SB) into the bound states consistently, so that the pion, although constructed as a quark-antiquark composite described by its Bethe-Salpeter (BS) bound-state vertex $\Gamma_\pi(p, k_\pi)$, also appears as a Goldstone boson in the chiral limit (k_π denotes the relative momentum of the quark and antiquark constituents of the pion bound state). Any dependence on what precisely the solutions for the dynamically dressed quark propagator

$$S(k) = \frac{1}{i\not{k}A(k^2) + m + B(k^2)} \equiv -i\not{k}\sigma_V(k^2) + \sigma_S(k^2) \quad (2)$$

and the BS vertex $\Gamma_\pi(p, k_\pi)$ are, drops out in the course of the analytical derivation of Eq. (1) in the chiral and soft limit. This is as it should be, because the amplitudes predicted by the anomaly (again in the chiral limit $m = 0 = m_\pi$ and the soft limit, *i.e.*, at zero four-momentum) are independent of the bound-state structure, so that the SD approach is the bound-state approach that correctly incorporates the Abelian axial anomaly.

The Abelian axial anomaly amplitudes in Eq. (1) are reproduced if the electromagnetic interactions are embedded in the context of the SD approach through the framework used, for example, by [5,4,6,3,8–10], and often called generalized impulse approximation (GIA) - *e.g.*, by [6,3,9,10]. There, the quark-photon-quark ($q\gamma q$) vertex $\Gamma_\mu(k, k')$ is dressed so that it satisfies the vector Ward-Takahashi identity (WTI) $(k' - k)_\mu \Gamma^\mu(k', k) = S^{-1}(k') - S^{-1}(k)$ together with the quark propagators (2), which are in turn dressed consistently with the solutions for the pion bound state BS vertices Γ_π . The box graph for $\gamma \rightarrow 3\pi$ in Fig. 1 is a GIA graph if all its propagators and vertices are dressed like this. Table 1 of Ref. [8] illustrates quantitatively the consequences of using the bare vertex γ^μ (which is WTI-violating in the context of the SD approach, instead of a WTI-preserving dressed $q\gamma q$ vertex) on the example of $\pi^0 \rightarrow \gamma\gamma$.

In practice, one usually uses [4,6,3,8–10] realistic WTI-preserving *Ansätze* for $\Gamma^\mu(k', k)$. Following AR [6], we employ the Euclidean form of the widely used Ball-Chiu [11] vertex, which is fully given in terms of the quark propagator functions of Eq. (2):

$$\Gamma^\mu(q', q) = [A(q'^2) + A(q^2)] \frac{\gamma^\mu}{2} + \frac{(q' + q)^\mu}{(q'^2 - q^2)} \{ [A(q'^2) - A(q^2)] \frac{(q' + q)^\mu}{2} - i[B(q'^2) - B(q^2)] \}. \quad (3)$$

The amplitude $T_\pi^{2\gamma}$ obtained in the chiral and soft limit is an excellent approximation for the realistic $\pi^0 \rightarrow \gamma\gamma$ decay. On the other hand, the already published [12] and presently planned Primakoff experiments at CERN [13], as well as the current CEBAF measurement of the $\gamma\pi^+ \rightarrow \pi^+\pi^0$ process [14] involve values of energy and momentum transfer sufficiently large to give a lot of motivation for theoretical predictions of the extension of the anomalous $\gamma \rightarrow 3\pi$ amplitude away from the soft point. In the present paper we follow essentially the approach of AR [6], the difference being precisely the way in which the $\gamma \rightarrow 3\pi$ form factor is extended beyond the soft point. We perform this extension guided by the insights from our Ref. [15].

2. Considering just one graph, for example Fig. 1, enabled Ref. [6] to reproduce analytically the anomalous amplitude (1) for $p_1 = p_2 = p_3 = 0$. However, computing the form factor $F_\gamma^{3\pi}$ beyond the soft limit requires careful inclusion of all six contributing graphs, obtained from Fig. 1 by the permutations of the vertices of the three different pions $\pi^a = \pi^+, \pi^0, \pi^-$. Otherwise, $F_\gamma^{3\pi}$ would not be properly symmetrical under $p_1 \leftrightarrow p_2 \leftrightarrow p_3$. In Fig. 1, as well as in the other five

associated graphs, the relative momenta of the constituents of the pion bound states, as well as the momenta flowing through the four sections of the quark loop, are conveniently given by various combinations of the symbols $\alpha, \beta, \gamma = +, 0, -$ in $k_{\alpha\beta\gamma} \equiv k + (\alpha p_1 + \beta p_2 + \gamma p_3)/2$.

If we denote the contribution of the first diagram in Fig. 1, by $-ie^\mu \epsilon_{\mu\nu\rho\sigma} p_1^\nu p_2^\rho p_3^\sigma f_\gamma^{3\pi}(p_1, p_2, p_3)$, where ϵ^μ is the photon polarization vector, the $\gamma \rightarrow 3\pi$ amplitude $\mathcal{A}_\gamma^{3\pi}$, *viz.*, the total scalar form factor $F_\gamma^{3\pi}(p_1, p_2, p_3)$ associated with it, is written as

$$\begin{aligned} \mathcal{A}_\gamma^{3\pi} &= -ie^\mu \epsilon_{\mu\nu\rho\sigma} p_1^\nu p_2^\rho p_3^\sigma F_\gamma^{3\pi}(p_1, p_2, p_3) \\ &= -ie^\mu \epsilon_{\mu\nu\rho\sigma} p_1^\nu p_2^\rho p_3^\sigma f_\gamma^{3\pi}(p_1, p_2, p_3) + [\text{all permutations of } \pi^+(p_1), \pi^0(p_2), \pi^-(p_3)]. \end{aligned} \quad (4)$$

In Ref. [15] we computed (4), *i.e.*, the form factor $F_\gamma^{3\pi}$, in the “free” quark loop (QL) model (and hence also the lowest order σ -model and chiral quark models) with the constant constituent mass M . In the SD approach, one instead has the momentum-dependent (Euclidean) quark mass function $M(p^2) \equiv B(p^2)/A(p^2)$. The functions $A(p^2)$ and $B(p^2)$, *i.e.*, the dressed quark propagators (2), are in principle the solutions of the appropriate SD equation. The quark-pion vertices $\Gamma_\pi(p, k_\pi)$ are the bound-state vertices obtained as the pion solutions of the BS equation consistently coupled with the SD equation for the quark propagator through the usage of its solution $S(p)$ and the same interaction (see [16] and references therein for an example thereof, and [1–3] for reviews and applications). This approach is therefore also often called the coupled SD-BS approach (*e.g.*, by [3,9,10]).

However, in the variant of the SD approach used by Roberts and Alkofer [4,6], they avoided solving the SD equation for the dressed quark propagator S by using a phenomenologically realistic *Ansatz* for the dressed quark propagator (2). In principle, one could invert such a propagator *Ansatz* and find out which interaction would give rise to it through the SD equation. Then, owing to working in the chiral *and* soft limit they also automatically obtained the solution of the BS equation. In this limit when the chiral symmetry is not broken explicitly by $m \neq 0$ but only dynamically and when pions must consequently appear as Goldstone bosons, the solution for the pion bound-state vertex Γ_π , corresponding to the Goldstone pion, is – to the order $\mathcal{O}(p^0)$ – given by the dressed quark propagator $S(k)$ (2). For the pion bound-state vertex Γ_π , Ref. [4,6] concretely used the solution, given in Eq. (5) immediately below, that is of zeroth order in the pion momentum p . This is appropriate close to the soft limit $p^\mu \rightarrow 0$. soft limit Γ_π fully saturates the Adler-Bell-Jackiw axial anomaly [5,4]. *In the chiral limit*, the pion decay constant f_π is found [17] to be equal to the normalization constant of Γ_π , whereas its $\mathcal{O}(p^0)$ piece is proportional to the chiral-limit solution for $B(k^2)$ from Eq. (2):

$$\Gamma_\pi(p^2 = -m_\pi^2 = 0; k) \equiv \Gamma_\pi(k) = \frac{B_0(k^2)}{f_\pi} \gamma_5. \quad (5)$$

The propagator function $B_0(k^2) \equiv B(k^2)_{m=0}$ is the one obtained in the chiral limit of the vanishing current quark mass m , where the quark constituent mass arises purely from D χ SB. Eq. (5) is analogous to the quark-level Goldberger-Treiman relation $g = M/f_\pi$ for “free” constituent quarks with the constant mass M . The constant quark-pion coupling strength g corresponds to $B_0(k^2)/f_\pi$ in the SD approach.

Since the pion is in a good approximation an (almost) massless Goldstone boson, we follow AR [4,6] in approximating the BS-vertex of the realistically massive pion by Eq. (5):

$$\Gamma_\pi(p^2 = -m_\pi^2 = -m_\pi^{*2}; k) \approx \Gamma_\pi(k). \quad (6)$$

The contribution of the single diagram Fig. 1, $-i\epsilon_{\mu\nu\rho\sigma} p_1^\nu p_2^\rho p_3^\sigma f_7^{3\pi}(p_1, p_2, p_3)$, is then

$$-\int \frac{d^4 k}{(2\pi)^4} \text{Tr} \left\{ i\epsilon Q \Gamma_\mu(k_{+++}, k_{---}) S(k_{---}) \sqrt{2} \tau_+ \Gamma_\pi(k_{--0}) \right. \\ \left. \times S(k_{--0}) \tau_3 \Gamma_\pi(k_{-0+}) S(k_{-0+}) \sqrt{2} \tau_- \Gamma_\pi(k_{0++}) S(k_{0++}) \right\}, \quad (7)$$

where the Pauli $SU(2)$ matrices τ_3 and $\tau_\pm = (\tau_1 \pm i\tau_2)/2$ correspond, respectively, to π^0 and emitted π^\mp (absorbed π^\pm). The quark charge matrix in the $SU(2)$ -isospin space is $Q \equiv \text{diag}[Q_u, Q_d] = \text{diag}[2/3, -1/3]$. For this particular diagram the isospin trace is $\text{Tr}(Q\tau_+\tau_3\tau_-) = (-1)Q_u = -2/3$. The color trace yields the factor N_c . The Dirac trace leads to the form

$$\text{Tr}\{\dots\} = T_1 \epsilon_{\mu\nu\rho\sigma} p_1^\nu p_2^\rho p_3^\sigma + T_3 k^\mu \epsilon_{\alpha\nu\rho\sigma} k^\alpha p_1^\nu p_2^\rho p_3^\sigma \\ + T_2 \epsilon_{\mu\nu\rho\sigma} k^\nu p_2^\rho p_3^\sigma + T_3 \epsilon_{\mu\nu\rho\sigma} p_1^\nu k^\rho p_3^\sigma + T_4 \epsilon_{\mu\nu\rho\sigma} p_1^\nu p_2^\rho k^\sigma, \quad (8)$$

where T_i 's are functions of scalar products $p_i \cdot p_j$ and $k \cdot p_j$ only ($i, j = 1, 2, 3$). They are integrals over the loop momentum k , given by lengthy integrands, so we do not present them explicitly. Obviously, evaluating $F_7^{3\pi}$ in the SD approach, is a harder task than in the context of our earlier Ref. [15] where the quark-pion coupling is constant instead of the present BS-vertex (5), and the quark propagator has a constant constituent mass, as opposed to Eq. (2). Nevertheless, it is possible to formulate an expansion in the pion momenta similar to that in Ref. [15]. The integrands of the T_i -functions ($i = 1, \dots, 5$) are expanded around the soft limit $p_i = 0$,

$$f(k, p_i) = f(k, 0) + \sum_i p_i^\mu \left[\frac{\partial f(k, p_i)}{\partial p_i^\mu} \right] \Big|_{p_i^\mu=0} + \frac{1}{2} \sum_{i,j} p_i^\mu p_j^\nu \left[\frac{\partial^2 f(k, p_i)}{\partial p_i^\mu \partial p_j^\nu} \right] \Big|_{p_i^\mu=0} + \dots \quad (9)$$

whereby the problem is reduced to evaluating integrals over the loop momentum k which contain in their integrands only functions of k^2 times powers of scalar products $k \cdot p_j$. The integrals with an odd number of k_μ factors vanish, while the integrals with an even number of k_μ 's are turned into integrals over pure functions of k^2 through symmetric integration, *i.e.*, by utilizing

$$\int k^\mu k^\nu f(k^2) d^4 k = \frac{g^{\mu\nu}}{4} \int k^2 f(k^2) d^4 k \quad (10)$$

$$\int k^\mu k^\nu k^\alpha k^\beta f(k^2) d^4 k = \frac{g^{\mu\nu} g^{\alpha\beta} + g^{\mu\alpha} g^{\nu\beta} + g^{\mu\beta} g^{\nu\alpha}}{24} \int (k^2)^2 f(k^2) d^4 k. \quad (11)$$

Conveniently defining

$$f_7^{3\pi}(p_1, p_2, p_3) \equiv -\frac{e N_c}{2\pi^2 f_\pi^3} \text{Tr}(Q\tau_+\tau_3\tau_-) J(p_1, p_2, p_3), \quad (12)$$

and analogously for the other diagrams, the $\gamma 3\pi$ form factor written as the sum over the six diagrams is

$$F_7^{3\pi}(p_1, p_2, p_3) = \frac{e N_c}{2\pi^2 f_\pi^3} \left(\frac{2}{3} \{ J(p_1, p_2, p_3) + J(p_1, p_3, p_2) + J(p_2, p_1, p_3) \} \right. \\ \left. - \frac{1}{3} \{ J(p_3, p_1, p_2) + J(p_3, p_2, p_1) + J(p_2, p_3, p_1) \} \right). \quad (13)$$

Owing to our expansion method, $J(p_1, p_2, p_3)$ and its companions with the permuted arguments p_1, p_2, p_3 , are given in terms of expansions in the scalar products of the external momenta p_1, p_2, p_3 , and the coefficients are given by integrals of functions (coming from the propagators and vertices) of the squared loop momenta $k^2 = \ell$. We evaluate these integrals in Euclidean space. For example, consider the lowest, zeroth order contribution to the expansion, $J(0, 0, 0)$, which determines the $\gamma 3\pi$ amplitude at the soft point. It is given by the loop integral

$$J(0, 0, 0) = \int_0^\infty d\ell \ell B_0(\ell)^3 \sigma_V(\ell)^2 [A(\ell) \sigma_S(\ell) \sigma_V(\ell) \\ + \frac{1}{2} \ell \sigma_S(\ell) \sigma_V(\ell) A'(\ell) - \frac{1}{2} \ell \sigma_V(\ell)^2 B'(\ell) - \frac{3}{2} \ell A(\ell) \sigma_V(\ell) \sigma_S'(\ell)]. \quad (14)$$

The two equivalent pairs of functions in the Euclidean quark propagator (2) are connected with each other through the relations

$$A(p^2) = \frac{\sigma_V(p^2)}{p^2 \sigma_V^2(p^2) + \sigma_S^2(p^2)}, \quad B(p^2) = \frac{\sigma_S(p^2)}{p^2 \sigma_V^2(p^2) + \sigma_S^2(p^2)} - m. \quad (15)$$

in our present convention, m is separated out of $B(p^2)$ which is thus purely dynamically generated in contrast to the convention we used previously [3] where the quark mass m which breaks chiral symmetry explicitly was lumped into $B(p^2)$. In the chiral limit, where not only $B_0(\ell)^3$ but all propagator functions (2) appearing in Eq. (14) correspond to the $m = 0$ case, AR [6] evaluated $J(0, 0, 0)$ analytically: its value in the chiral limit, $J_0 \equiv J_0(0, 0, 0)$, is always $J_0 = 1/6$ irrespectively of what the functions defining the quark propagator (2) and the pion BS vertex (5) concretely are. This enabled AR to prove that, remarkably, the SD approach exactly reproduces the soft-point amplitude (1) independently of details of bound state structure. Thus, this bound-state approach consistently incorporates not only the "triangle", but also the "box" axial anomaly.

Since $J(0, 0, 0)$ is equal in every diagram, and in the chiral limit it is always $J_0 = 1/6$, our sum over diagrams (13) also reproduces the chiral-limit result (1) for $F_7^{3\pi}(0, 0, 0)$.

Same as in Ref. [15], we found having the sum of diagrams essential for obtaining the correct $\gamma 3\pi$ amplitude beyond the soft point, where different diagrams contribute different combinations of powers of the scalar products $p_i \cdot p_j$. To get $F_7^{3\pi}(p_1, p_2, p_3)$ symmetric under the interchange of the three external momenta, one needs to consider the sum of at least three graphs corresponding to one of the combinations enclosed in the curly brackets in Eq. (13). As in the simpler case of the "free" constituent quark loop calculation, these curly brackets are equal to each other.

3. Unlike J_0 , the expansion coefficients of terms beyond soft and chiral limits are not independent on the internal structure of the pion. To evaluate the integrals giving them, we must specify the propagator functions in Eqs. (2) and (5). We adopt the AR quark propagator *Ansatz* supposedly suitable for modeling confined quarks [6], namely

$$\bar{\sigma}_S(x) = C_m e^{-2x} + 2\bar{m} \frac{1 - e^{-2(x+\bar{m}^2)}}{2(x+\bar{m}^2)} + \frac{1 - e^{-b_1 x}}{b_1 x} + \frac{1 - e^{-b_2 x}}{b_2 x} \left(b_0 + b_2 \frac{1 - e^{-\epsilon x}}{\epsilon x} \right), \quad (16)$$

$$\bar{\sigma}_V(x) = \frac{2(x+\bar{m}^2) - 1 + e^{-2(x+\bar{m}^2)}}{(x+\bar{m}^2)^2} - \bar{m} C_m e^{-2x}, \quad (17)$$

where the dimensionless functions $\bar{\sigma}_S(x)$ and $\bar{\sigma}_V(x)$ are related to the scalar and vector propagator functions through the characteristic mass scale $\Lambda = \sqrt{2D}$:

$$\bar{\sigma}_S(x) = \sqrt{2D} \sigma_S(k^2), \quad \bar{\sigma}_V(x) = 2D \sigma_V(k^2), \quad (18)$$

along with the quark momentum and mass, $k^2 = \ell \equiv 2D x$ and $\bar{m} = m/\sqrt{2D}$.

The above quark propagator *Ansätze*, together with the chiral-limit pseudoscalar BS vertex (5), define the model of the quark substructure of the light pseudoscalar meson – the pion. By fitting a considerable number of pion observables (see Table 1 in Ref. [6]), the parameters were fixed to the values

$$\begin{array}{lll} C_m = 0.121 & \bar{m} = 0 & \leftarrow \text{in the chiral limit} \\ C_m = 0 & \bar{m} = 0.00897 & \leftarrow \text{for massive quarks} \\ b_0 = 0.131 & b_1 = 2.90 & \epsilon = 10^{-4} \\ b_2 = 0.603 & b_3 = 0.185 & D = 0.16 \text{ GeV}^2. \end{array} \quad (19)$$

We present our expansion around the soft point by re-writing the (dimensionful) expansion coefficients in terms of dimensionless numbers divided by the appropriate power of a characteristic mass scale Λ . In the free constituent quark loop calculation [15], this scale was of the order of the constituent quark mass M . In the present model, it is obviously $\Lambda = \sqrt{2D} = 565.69 \text{ MeV}$. After introducing the form factor normalized to the anomaly amplitude (1), $\bar{F}_7^{3\pi}(p_1, p_2, p_3) \equiv F_7^{3\pi}(p_1, p_2, p_3)/F_7^{3\pi}(0, 0, 0)$, our expansion for *general, possibly off-shell impulses* p_i , to the order $\mathcal{O}(p^4)$ becomes

$$\begin{aligned} \bar{F}_7^{3\pi}(p_1, p_2, p_3) = & 0.96274 - \frac{0.94952}{\Lambda^2} (p_1 \cdot p_2 + p_1 \cdot p_3 + p_2 \cdot p_3) - \frac{0.84175}{\Lambda^2} (p_1^2 + p_2^2 + p_3^2) \\ & + \frac{0.63155}{\Lambda^4} ((p_1 \cdot p_2)^2 + (p_1 \cdot p_3)^2 + (p_2 \cdot p_3)^2) \\ & + \frac{0.76839}{\Lambda^4} (p_1^2 p_2^2 + p_1^2 p_3^2 + p_2^2 p_3^2) + \frac{0.44218}{\Lambda^4} (p_1^4 + p_2^4 + p_3^4) \\ & + \frac{1.02189}{\Lambda^4} (p_1 \cdot p_2 p_1 \cdot p_3 + p_1 \cdot p_2 p_2 \cdot p_3 + p_1 \cdot p_3 p_2 \cdot p_3) \\ & + \frac{0.97567}{\Lambda^4} (p_1^2 p_1 \cdot p_2 + p_1^2 p_1 \cdot p_3 + p_2^2 p_1 \cdot p_2 + p_2^2 p_2 \cdot p_3 + p_3^2 p_1 \cdot p_3 + p_3^2 p_2 \cdot p_3) \\ & + \frac{0.83507}{\Lambda^4} (p_1^2 p_2 \cdot p_3 + p_2^2 p_1 \cdot p_3 + p_3^2 p_1 \cdot p_2) + \mathcal{O}(p^6). \end{aligned} \quad (20)$$

Since this was obtained with the propagators in the presence of a small ($\bar{m} = 0.00897$) explicit chiral symmetry breaking, the zeroth-order term [$6J(0, 0, 0) = 0.96274$] slightly differs from 1. Note the difference with respect to the simpler “free” quark loop case [15], where the zeroth-order term $6J(0, 0, 0) = 1$ always. For the chiral quark propagators,

$$\begin{aligned} \bar{F}_7^{3\pi}(p_1, p_2, p_3)_0 = & 1 - \frac{0.92228}{\Lambda^2} (p_1 \cdot p_2 + p_1 \cdot p_3 + p_2 \cdot p_3) - \frac{0.83476}{\Lambda^2} (p_1^2 + p_2^2 + p_3^2) \\ & + \frac{0.54703}{\Lambda^4} ((p_1 \cdot p_2)^2 + (p_1 \cdot p_3)^2 + (p_2 \cdot p_3)^2) \\ & + \frac{0.70561}{\Lambda^4} (p_1^2 p_2^2 + p_1^2 p_3^2 + p_2^2 p_3^2) + \frac{0.40287}{\Lambda^4} (p_1^4 + p_2^4 + p_3^4) \\ & + \frac{0.88247}{\Lambda^4} (p_1 \cdot p_2 p_1 \cdot p_3 + p_1 \cdot p_2 p_2 \cdot p_3 + p_1 \cdot p_3 p_2 \cdot p_3) \end{aligned}$$

$$\begin{aligned} & + \frac{0.86649}{\Lambda^4} (p_1^2 p_1 \cdot p_2 + p_1^2 p_1 \cdot p_3 + p_2^2 p_1 \cdot p_2 + p_2^2 p_2 \cdot p_3 + p_3^2 p_1 \cdot p_3 + p_3^2 p_2 \cdot p_3) \\ & + \frac{0.74448}{\Lambda^4} (p_1^2 p_2 \cdot p_3 + p_2^2 p_1 \cdot p_3 + p_3^2 p_1 \cdot p_2). \end{aligned} \quad (21)$$

In the both cases, note the total symmetry in the interchange of the momenta p_1, p_2, p_3 . To elucidate the effect of this symmetry on the momentum dependence of the $\gamma 3\pi$ form factor, we re-express the scalar products $p_i \cdot p_j$ through the Mandelstam variables. We use the definitions of Ref. [6], which is the Euclidean version of the definitions in Ref. [14]: $s = -(p_1 + p_2)^2 \equiv m_\pi^2 \bar{s}$, $t' = -(p_2 + p_3)^2 \equiv m_\pi^2 \bar{t}'$, $u = -(p_1 + p_3)^2 \equiv m_\pi^2 \bar{u}$, while $t = -p_3^2 \equiv m_\pi^2 \bar{t}$ serves as the measure of the virtuality of the third pion which is off shell in the CEBAF experiment [14].

On the other hand, in all three pertinent experiments [12, 14, 13], the first two pions are on shell. We can thus specialize to $p_1^2 = p_2^2 = -m_\pi^2$ and obtain more compact expressions for the $\mathcal{O}(p^4)$ amplitudes in terms of Mandelstam variables. For massive quarks eq. (20) then becomes

$$\begin{aligned} \bar{F}_7^{3\pi}(s, t', u) = & \left(0.96274 - \frac{0.21554 m_\pi^2}{\Lambda^2} + \frac{0.11534 m_\pi^4}{\Lambda^4} \right) \\ & + \left(\frac{0.47476}{\Lambda^2} - \frac{0.17682 m_\pi^2}{\Lambda^4} \right) (s + t' + u) + \frac{0.15789}{\Lambda^4} (s^2 + t'^2 + u^2) \\ & + \frac{0.25547}{\Lambda^4} (st' + t'u + su) - \frac{0.08341}{\Lambda^4} (s + t' + u)t \\ & - \left(\frac{0.10777}{\Lambda^2} - \frac{0.07967 m_\pi^2}{\Lambda^4} \right) t + \frac{0.03776}{\Lambda^4} t^2 + \frac{0.01000 m_\pi^2}{\Lambda^4} (m_\pi^2 - t)s. \end{aligned} \quad (22)$$

Similarly, in the chiral limit of vanishing m_π , where $p_1^2 = p_2^2 = 0$, the amplitude (21) becomes

$$\begin{aligned} \bar{F}_7^{3\pi}(s, t', u)_0 = & 1 + \frac{0.46114}{\Lambda^2} (s + t' + u) + \frac{0.13676}{\Lambda^4} (s^2 + t'^2 + u^2) \\ & + \frac{0.22062}{\Lambda^4} (st' + t'u + su) - \frac{0.06089}{\Lambda^4} (s + t' + u)t \\ & - \frac{0.08752}{\Lambda^2} t + \frac{0.03052}{\Lambda^4} t^2 - \frac{0.00811}{\Lambda^4} ts. \end{aligned} \quad (23)$$

In both cases, we isolated in the last term the violation of the $s \leftrightarrow t' \leftrightarrow u$ symmetry, which occurs when the third pion is off shell, $t \neq m_\pi^2$ (or $t \neq 0$ in the chiral case).

We indicated only the s, t', u dependence of the amplitudes, since t is of course not independent because of the constraint $s + t' + u = -p_1^2 - p_2^2 - p_3^2 - q^2$, where $q = p_1 + p_2 + p_3$ is the photon momentum. One can take the photon to be on shell in all three pertinent $\gamma 3\pi$ experiments [12, 14, 13]. We thus set $q^2 = 0$ in addition to $p_1^2 = p_2^2 = -m_\pi^2$, whereby the above kinematical constraint becomes

$$s + t' + u = 2m_\pi^2 + t. \quad (24)$$

In any case, this constraint (24) dictates that the $\mathcal{O}(p^2)$ -terms, since they appear in the appropriate symmetric combination, contribute only to the part independent of s, t' and u . This contribution is in fact constant (of the order of m_π^2) up to t , the virtuality of the third pion. Therefore, the main contribution to the term linear in s, t' and u (dominating the s, t', u -dependence around the soft

limit), comes from $\mathcal{O}(p^4)$ and not $\mathcal{O}(p^2)$. The coefficients of the linear and quadratic terms will thus be comparably small, giving the parabolic shape to the curves displaying our form factors, instead of the steep linear appearance [6] due to spurious, relatively large linear terms (suppressed only as $1/\Lambda^2$) which come from $\mathcal{O}(p^2)$ when there is no symmetry under the interchange of the pion momenta [so that the constraint (24) cannot do its job].

4. The experiment which provided the only presently existing data point [12] and the one planned at CERN [13], belong to the Primakoff type, where also the third pion is on its mass shell, fixing $t = m_\pi^2 \bar{t} = m_\pi^2$. We then get, in terms of the Mandelstam variables expressed in terms of pion mass squared,

$$\bar{F}_\gamma^{3\pi}(s, t') = 1.0319 - 0.00065(\bar{s} + \bar{t}') + 0.00022(\bar{s}^2 + \bar{s}\bar{t}' + \bar{t}'^2), \quad (25)$$

while in the chiral limit, where on shell means $\bar{t} = 0$,

$$\bar{F}_\gamma^{3\pi}(s, t')_0 = 1 + 0.000190(\bar{s}^2 + \bar{s}\bar{t}' + \bar{t}'^2). \quad (26)$$

For the second variable fixed to $\bar{t}' = -1$, Eqs. (25) and (26) are depicted, respectively, by solid and short-dashed curves in Fig. 2.

In the CEBAF measurement [14], the third pion has spacelike virtuality of the order $t \approx -m_\pi^2$, so we also give $\bar{F}(s, t')$ obtained by fixing $\bar{t} = -1$:

$$\bar{F}(s, t') = 0.98524 - 0.00015\bar{s} - 0.00022\bar{t}' + 0.00022(\bar{s}^2 + \bar{s}\bar{t}' + \bar{t}'^2), \quad (27)$$

and again with $\bar{t} = -1$, but in the chiral limit,

$$\bar{F}_\gamma^{3\pi}(s, t')_0 = 0.97799 + 0.00022\bar{s} + 0.00019\bar{t}' + 0.000190(\bar{s}^2 + \bar{s}\bar{t}' + \bar{t}'^2). \quad (28)$$

CEBAF aims [14] to measure the s -dependence of the $\gamma 3\pi$ form factor in the interval $s \in [4m_\pi^2, 16m_\pi^2]$, with such kinematics that $\bar{t}' = -1$ is a good choice for fixing the remaining variable (as we explained in Ref. [15]). We thus depict Eqs. (27) and (28) for $t' = -m_\pi^2$ by respective solid and short-dashed curves in Fig. 3.

In Figs. 2 and 3 we also compare our results with some other theoretical predictions for $t = m_\pi^2$ and $t = -m_\pi^2$, respectively. The dash-dotted lines represent the chiral perturbation theory (χ PT) form factor [18] (with Holstein's [19] choice of renormalization – *i.e.*, we take his [19] Eq. (10) for the χ PT prediction). The dotted curves are the vector meson dominance (VMD) form factors [20] [*i.e.*, Holstein's [19] Eq. (9) for $t = \pm m_\pi^2$].

All depicted theoretical form factors indicate that the existing data point [12] is probably an overestimate. In the considered s -interval, the prediction of the present model is lower than those of VMD and χ PT. The current CEBAF measurement [14] should be accurate enough to discriminate between at least some of these results.

The most instructive comparison of theoretical predictions is the one with the form factors calculated from the box graph with the ordinary (“free”) constituent quarks looping inside [15]. In both Fig. 2 and Fig. 3, they are given by the long-dashed curve, the line of empty squares and the line of crosses, for the constant constituent masses M of 330 MeV ($\approx M_{nucleon}/3$), 400 MeV ($= \sqrt{D}$) and 580 MeV ($\approx \sqrt{2D}$), respectively. Besides the graphs, one should also compare the expressions (22), (23) for the expansions in the powers of scalar momenta $p_i \cdot p_j$ in the present case

with their analogy in our previous paper [15]. One can conclude that for the presently experimentally interesting momenta, the present model and the simple “free” constituent quark loop model agree quite well as long as the mass scale of these models is similar, $\sqrt{2D} \sim M$. The present SD model, with its dressed propagators and vertices, does have faster changing $F_\gamma^{3\pi}(s)$ than the simple constituent quark loop model (for the approximately same mass scale, *i.e.* $\sqrt{2D} \approx M$), but this is at the presently considered momenta compensated by the larger constant term in the latter model. While we can conclude that in the case of this particular form factor, the present SD model does not bring in the present application novel features with respect to the simple constituent quark loop model as far as the magnitude of the form factor is concerned, we can say that considering these two models led to a fairly complete understanding of the quark box graph calculation of the anomalous $\gamma 3\pi$ form factor. On the other hand, because of that understanding, the experiment can bring an important new input to the SD modeling. If the experimental form factor is measured at CEBAF with sufficient precision to judge the present SD model results too low, it will be an unambiguous signal that the SD modeling should be reformulated and refitted so that it is governed by a smaller mass scale.

ACKNOWLEDGMENTS

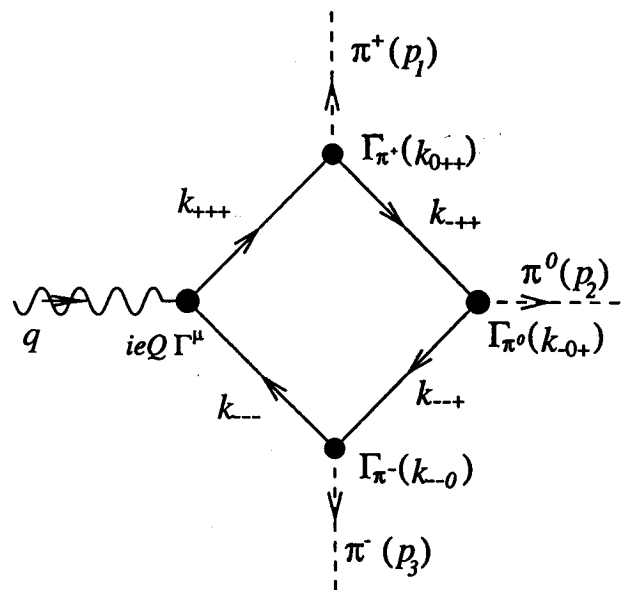
The authors thank R. Alkofer and D. Kekez for many helpful discussions, K. Kumerički for checking the manuscript, and Physics Department of Bielefeld University for hospitality during work on a substantial part of this paper. This work was supported by the Croatian Ministry of Science and Technology contract 1-19-222, and in part (B. B.) by the U.S. Department of Energy under Contract No. DE-AC05-84ER40150 and Grant No. DE-FG-5-94ER40832.

REFERENCES

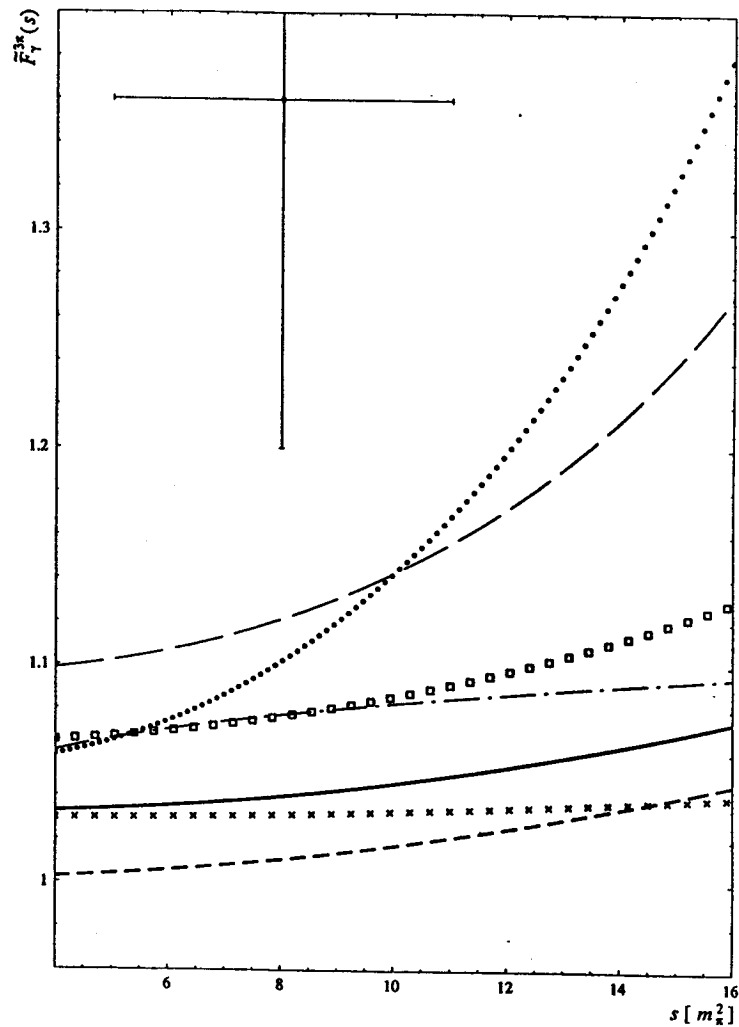
- [1] C. D. Roberts, Nonperturbative QCD with modern tools, Summary of three lectures given at 11th Physics Summer School on Frontiers in Nuclear Physics: From Quark - Gluon Plasma to Supernova, Canberra, Australia, 12-23 Jan 1998. e-Print Archive: nucl-th/9807026.
- [2] C.D. Roberts and A.G. Williams, *Prog. Part. Nucl. Phys.* 33 (1994) 477.
- [3] D. Kekez, B. Bistronić, and D. Klabučar, *Int. J. Mod. Phys. A* 14, (1999) 161.
- [4] C. D. Roberts, *Nucl. Phys. A* 605 (1996) 475; C. D. Roberts, in: *Chiral Dynamics: Theory and Experiment*, eds. A M Bernstein and B R Holstein, *Lecture Notes in Physics*, Vol. 452, Springer, Berlin, 1995 p. 68.
- [5] M. Bando, M. Harada, and T. Kugo, *Prog. Theor. Phys.* 91 (1994) 927.
- [6] R. Alkofer and C. D. Roberts, *Phys. Lett.* B369 (1996) 101.
- [7] S. L. Adler, B. W. Lee, S. Treiman, and A. Zee, *Phys. Rev. D* 4 (1971) 3497 (1971); M. V. Terent'ev, *Phys. Lett.* 38B (1972) 419; R. Aviv and A. Zee, *Phys. Rev. D* 5 (1972) 2372.
- [8] D. Kekez and D. Klabučar, *Phys. Lett.* B387 (1996) 14.
- [9] D. Klabučar and D. Kekez, *Phys. Rev. D* 58 (1998) 096003.
- [10] D. Kekez and D. Klabučar, *Phys. Lett. B* 457 (1999) 359.
- [11] J. S. Ball and T.-W. Chiu, *Phys. Rev. D* 22 (1980) 2542.
- [12] Yu. M. Antipov *et al.*, *Phys. Rev. D* 36 (1987) 21.
- [13] M. A. Moinester, V. Steiner, and S. Prakhov, *Hadron-Photon Interactions in COMPASS*, to be published in the proceedings of 37th International Winter Meeting on Nuclear Physics, Bormio, Italy, 25-29 Jan 1999, e-print hep-ex/9903017.
- [14] R. A. Miskimen, K. Wang, and A. Yagneswaran (spokesmen), Study of the Axial Anomaly using the $\gamma\pi^+ \rightarrow \pi^+\pi^0$ Reaction Near Threshold, Letter of intent, CEBAF-experiment 94-015.
- [15] B. Bistronić and D. Klabučar, Quark loop calculation of the $\gamma \rightarrow 3\pi$ form factor, e-Print Archive: hep-ph/9907515, to appear in *Phys. Rev. D* (2000).
- [16] P. Jain and H. J. Munczek, *Phys. Rev. D* 48 (1993) 5403.
- [17] R. Jackiw and K. Johnson, *Phys. Rev. D* 8 (1973) 2386.
- [18] J. Bijnens, A. Bramon, and F. Cornet, *Phys. Lett.* B237 (1990) 488.
- [19] B. Holstein, *Phys. Rev. D* 53 (1996) 4099.
- [20] S. Rudaz, *Phys. Lett.* B145 (1984) 281; T.D. Cohen, *Phys. Lett.* B233 (1989) 467.

FIGURE CAPTIONS

- Fig. 1: One of the six box diagrams for the process $\gamma \rightarrow \pi^+\pi^0\pi^-$. Within the scheme of generalized impulse approximation, the propagators and vertices are dressed. The position of the u and d quark flavors on the internal lines, as well as Q_u or Q_d quark charges in the quark-photon vertex, varies from graph to graph, depending on the position of the quark-pion vertices.
- Fig. 2: Various predictions for the s -dependence of the normalized $\gamma 3\pi$ form factor. We compare the form factor obtained by us with AR Ansätze [6] for both $m_\pi = 138.5$ MeV (solid curve) and the chiral limit ($m_\pi = 0$, dashed curve), with the predictions of the vector meson dominance [20] (dotted curve), chiral perturbation theory [18,19] (dash-dotted curve), and quark loop model [15] for $M = 330$ MeV (long-dashed curve), $M = 400$ MeV (boxes), and $M = 580$ MeV (crosses), and with the experimental data point [12], for all the pions on-shell and $t' = -m_\pi^2$.
- Fig. 3: The comparison of the $\gamma 3\pi$ form factor obtained by us with AR Ansätze [6] for both $m_\pi = 138.5$ MeV (solid curve) and the chiral limit ($m_\pi = 0$, dashed curve), with the predictions of the vector meson dominance [20] (dotted curve), chiral perturbation theory [18,19] (dash-dotted curve), and quark loop model [15] for $M = 330$ MeV (long-dashed curve), $M = 400$ MeV (boxes), and $M = 580$ MeV (crosses), for two of the pions on-shell and the third off-shell so that $t = -m_\pi^2$. (The Serpukhov data point [12] is also shown although it corresponds to all three pions on-shell.) The remaining variable is again fixed to $t' = -m_\pi^2$.



12



13

